Available online at www.sciencedirect.com
SCIENCE DIRECT®
Journal of Chromatography A, 1069 (2005) 65–77
JOURNAL OF CHROMATOGRAPHY A
www.elsevier.com/locate/chroma

Comparison of chromatographic ion-exchange resins IV. Strong and weak cation-exchange resins and heparin resins

Arne Staby[a,*], Maj-Britt Sand[a], Ronni G. Hansen[b], Jan H. Jacobsen[c], Line A. Andersen[d], Michael Gerstenberg[d], Ulla K. Bruus[a], Inge Holm Jensen[a]

[a] *Novo Nordisk A/S, Health Care Discovery and Development, Protein Separation, Hagedornsvej 1, DK-2820 Gentofte, Denmark*
[b] *Diabetes Bulk Production, Kalundborg, Denmark*
[c] *QA Fermentation and Recovery, Kalundborg, Denmark*
[d] *Novo Nordisk A/S, Sensor Technologies, Brennum Park, DK-3400 Hillerød, Denmark*

Available online 19 December 2004

Abstract

A comparative study was performed on heparin resins and strong and weak cation exchangers to investigate the pH dependence, efficiency, binding strength, particle size distribution, static and dynamic capacity, and scanning electron microscopy pictures of chromatographic resins. The resins tested include: Heparin Sepharose FF, SP Sepharose FF, CM Sepharose FF, Heparin Toyopearl 650m, SP Toyopearl 650m, CM Toyopearl 650m, Ceramic Heparin HyperD M, Ceramic S HyperD 20, and Ceramic CM HyperD F. Testing was performed with four different proteins: anti-FVII Mab (IgG), aprotinin, lysozyme, and myoglobin. Dependence of pH on retention was generally very low for proteins with high isoelectric point (p*I*), though some decrease of retention with increasing pH was observed for CM Ceramic HyperD F and S Ceramic HyperD 20. Binding of anti-FVII Mab with p$I < 7.5$ was observed on several resins at pH 7.5. Efficiency results show the expected trend of increasing dependence of the plate height with increasing flow rate of Ceramic HyperD resins followed by Toyopearl 650m resins and the highest flow dependence of the Sepharose FF resins corresponding to their pressure resistance. Determination of particle size distribution by two independent methods, coulter counting and SEM, was in good agreement. Binding strength of cation-exchange resins as a function of ionic strength varies depending on the protein. Binding and elution at high salt concentration may be performed with Ceramic HyperD resins, while binding and elution at low salt concentration may be performed with model proteins on heparin resins. Employing proteins with specific affinity for heparin, a much stronger binding is observed, however, some cation exchangers may still be good substitutions for heparin resins. Dynamic capacity at 10% breakthrough compared to static capacity measurements and dynamic capacity displays that approximately 40–80% of the total available capacity is utilized during chromatographic operation depending on flow rate. A general good agreement was obtained between results of this study and data obtained by others. Results of this study may be used in the selection of resins for testing during protein purification process development.

Keywords: Dynamic capacity; Heparin; Ion exchange; Preparative chromatography; Proteins; Static capacity; Stationary phases; LC

1. Introduction

In the pharmaceutical industry, speed to market is of main importance for all projects including protein and peptide products derived from recombinant sources. For the preparative purification of these recombinant proteins and peptides, ion-exchange chromatography and affinity chromatography have been standard techniques for many years. The popularity of ion-exchange chromatography is due to the simple methodology with preservation of biological activity of the proteins and peptides during processing, while affinity chromatography is a very powerful tool for removal of host cell related impurities and in many cases, inactive forms, etc. of

* Corresponding author. Tel.: +45 44 43 99 89; fax: +45 44 43 84 00.
E-mail address: ast@novonordisk.com (A. Staby).

0021-9673/$ – see front matter © 2004 Elsevier B.V. All rights reserved.
doi:10.1016/j.chroma.2004.11.094

the target molecule. Comparison of chromatographic resins is performed during process development, but due to time constraints only a limited number of resins is regularly tested for the specific application, and the results of such resin comparisons are rarely published. Affinity resins, like heparin resins, are usually more expensive than ion-exchange resins, thus the industry will seek to replace affinity resins with other resins, including ion-exchange resins, if possible.

Heparin affinity resins are widely used in purification of various proteins with a specific affinity for heparin, including blood proteins like factor IX [1] and anti-thrombin [2], and brain proteins like basic fibroblast growth factor [3] and many others [4]. Heparin resins for the purification of anti-thrombin III was recently presented by Nakamura et al. [5] comparing static binding capacities, purification performance, and caustic stability for five different resins.

A number of papers comparing cation exchangers has been published by commercial suppliers and non-commercial authors [6–32] comparing various chromatographic parameters including: dynamic [7,10–12,14,20,21,24,27,28], static [7,8,11,16,21,28], and ionic [7–11,16,27,30] capacities, binding strength [9,15,20,22–25,27,31,32], elution dependence on pH [13,15,19,20,22,23], efficiency [11,14,15,17,19,22,27,28,30], resolution [7,8,10–12,16,19,20,22,24–29], adsorption isotherms [11,18,21,23], pressure drop [10,11,16,19,22,28], compressibility [8,10,11,19], protein recovery [8,10,11,19,22], operating flow rate [8,10,11,14], cost, etc. [10,29], chemical stability [10,16,19,22], base matrix chemistry [7,9,16,18,19,22,28,29], pore size distribution [6,9,14,22], and others. The number of resins compared in these papers is typically two to four, however, the papers of DePhillips and Lenhoff [6,9,31], Boschetti [7], Levison et al. [8], Noel and Proctor [10], Nash and Chase [11], Chang and Lenhoff [18], and our group [33] include more than four cation exchangers. The test proteins used are typically lysozyme, chymotrypsinogen, cytochrome *c*, IgG and others.

This work is part of a continuing study performed at Novo Nordisk to characterize and compare commercial ion exchangers for improved selection for testing in process development. We have previously published the results of 17 strong anion-exchange resins and 7 strong cation-exchange resins comparing various chromatographic parameters by a systematic and consistent experimental setup [33–35]. The scope of this paper is to compare strong and weak cation exchangers from three different suppliers, that is, resins with ligates containing a sulphonic acid or carboxylic acid groups. In this comparison, we also include the corresponding three heparin resins, because they have pronounced similarity with cation exchangers, containing three sulphonic acid groups and one carboxylic acid group per heparin unit (see Fig. 1). The comparison include data on efficiency, binding strength, pH dependence, particle size distribution, dynamic and static capacity, and scanning electron microscopy (SEM) pictures of the resins performed at the same, relevant conditions. The four-test proteins used cover a broad range of isoelectric

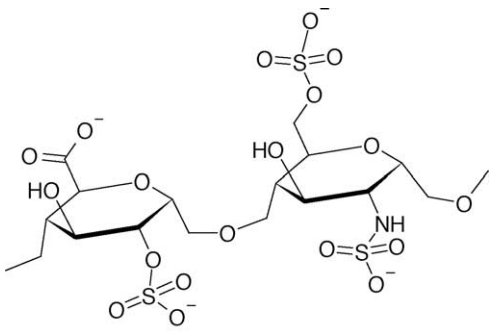

Fig. 1. Structure of heparin.

points and molecular weights with no specific affinity against heparin. They include both standard test proteins (lysozyme and myoglobin) and a protein and a peptide obtained at Novo Nordisk (anti-FVII Mab (IgG) [36] and aprotinin [37]). The difference in binding strength for heparin resins when used as an ion-exchanger and as an affinity resin was illustrated employing heparin binding protein (HBP) [38]. The study represents more than 1200 experimental measurements.

2. Experimental

2.1. Materials

Heparin Sepharose FF, SP Sepharose FF, and CM Sepharose FF beads were kindly donated by GE Healthcare (Uppsala, Sweden). Heparin Toyopearl 650m, SP Toyopearl 650m, and CM Toyopearl 650m beads were kindly donated by Tosoh Biosep (Stuttgart, Germany). Heparin Ceramic HyperD M, S Ceramic HyperD 20, CM Ceramic HyperD F, and S Ceramic HyperD F beads were kindly donated by Ciphergen (Cergy-Saint-Christophe, France).

Chicken egg white lysozyme (L6876) and horse skeletal muscle myoglobin (M0630) were purchased from Sigma (St. Louis, MO, USA). The industrial proteins/peptides in pure state and in real feed-stock (anti-FVII Mab, aprotinin, and HBP) were obtained from Novo Nordisk (Bagsværd, Denmark).

2-(*N*-Morpholino)ethanesulphonic acid (MES, M8250) and *N*-(2-hydroxyethyl)piperazine-*N*′-(2-ethanesulphonic acid) (HEPES, H3375) were purchased from Sigma. Sodium acetate (1.06267) and other chemicals: sodium chloride, hydrochloric acid, and acetone were analytical reagent grade and purchased from Merck (Darmstadt, Germany).

2.2. Instrumentation

A BioCAD Workstation from PE Biosystems (Cambridge, MA, USA) was used for chromatographic measurements. The standard BioCAD Workstation was equipped with a 100 μl sample injection loop, a 0.6 cm flow cell, pump heads for flow rates between 0.2 and 60 ml/min, and mixing of

standard buffer solutions (standard BioCAD buffer setup) was obtained through a mixing valve. UV detection was operated at 280 nm. The BioCAD was placed in a temperature controlled airbath from Brønnum (Herlev, Denmark) to maintain a constant temperature of 22 ± 1 °C throughout the measurements. UV–vis spectrophotometry for sample concentration adjustment was carried out on a HP8452A (Birkerød, Denmark).

Ceramic S HyperD 20 was packed at medium pressure in a 10 cm × 0.46 cm i.d. OmegaChrom PEEK column from Upchurch (Oak Harbor, WA, USA). Other chromatographic resins were packed in HR 5/10 columns (10 cm × 0.5 cm i.d.) supplied by GE Healthcare (Uppsala, Sweden).

Measurement of absorbance at 280 nm (A_{280}) for static capacity determination was performed using a diode array spectrophotometer 8452A from Hewlett-Packard (Palo Alto, CA, USA).

Coulter counting for particle size distribution measurement was performed using a Coulter Multisizer and sampling stand model S ST II from Coulter Electronics (Luton, UK).

SEM was carried out using a FEI Quanta 200 scanning electron microscope from FEI Co. (Hillsboro, USA).

2.3. Methods

The methods used in this study are equal to those of our previous experiments [34,35]. The resin comparison experiments were performed employing similar conditions, that is, the same scale, buffers, buffer concentration, temperature, protein concentration, solution conductivity, pH, gradients, and corresponding flow rates, where appropriate. Experiments were made in duplicate. The pH of buffer and protein/peptide solutions was adjusted with hydrochloric acid or sodium hydroxide. The following general methodology was used.

The column was equilibrated with a sufficient number of column volumes (CVs) of buffer (15–20 CVs). Samples of 1 mg/ml pure protein solutions were applied through the injection system or in case of frontal analysis experiments through the pump. Lysozyme and myoglobin freeze-dried products were dissolved directly in equilibration buffer pH 5.5 for frontal analysis experiments and in water for other experiments. Freeze-dried aprotinin was dissolved in water pH 5.5 for all experiments. Anti-FVII Mab was obtained at a concentration of 2 mg/ml in a 50 mM Tris + 100 mM NaCl, pH 8.0 solution, which was diluted with one volume of water and adjusted to pH 5.5 for all experiments. Properties of the test proteins are given in Table 1. In all experiments a standard buffer solution concentration of 16.7 mM MES + 16.7 mM HEPES + 16.7 mM sodium acetate was used. Column regeneration was performed with 5 CVs of 1.0 M NaCl in binding strength and frontal analysis experiments.

Table 1
Properties of test proteins

Protein	p*I*	Molecular mass ($\times 10^{-3}$)
Anti-FVII Mab (IgG)	∼6–7	150
Aprotinin	∼10.5	6
Lysozyme	∼11	14
Myoglobin	7–8	18
Heparin binding protein (HBP)	∼9	28

Packing of columns was performed according to manufacturer specifications. Properties of the heparin and cation-exchange resins and flow rates applied in these studies are presented in Table 2. Recommended maximum operating pressure/flow rate were obtained from the suppliers. The general flow rate used for pH dependence and binding strength measurements was approximately 50% of the recommended maximum operating flow rate/pressure. The low and high flow rates used for dynamic capacity determinations were approximately 25 and 75%, respectively, of the recommended maximum operating flow rate/pressure.

Extra column volume measurements of the system were performed as described elsewhere [34].

Table 2
Properties of the chromatographic heparin and cation-exchange resins and applied flow rates

Resin	Particle size (μm), supplier data	Mean particle size (μm), coulter counting	Mean particle size (μm), SEM	Maximum recommended pressure (bar)	Applied flow rates (ml/min)		
					General	Capacity, low	Capacity, high
Heparin Sepharose FF	90 (45–165)	67	46 (30–73)	3	1.2	0.6	1.8
SP Sepharose FF	90 (45–165)	–	52 (30–82)	3	1.2	0.6	1.8
CM Sepharose FF	90 (45–165)	57	45 (24–62)	3	1.2	0.6	1.8
Heparin Toyopearl 650m	65 (40–90)	–	–	5	0.8	0.5	1.3
SP Toyopearl 650m	65 (40–90)	62	51 (38–69)	5	0.8	0.5	1.3
CM Toyopearl 650m	65 (40–90)	62	50 (38–69)	5	0.8	0.5	1.3
Heparin Ceramic HyperD M	80	75	77 (62–95)	70	8.0	4.0	12.0
S Ceramic HyperD 20	20	–	19 (14–27)	200	10.0	2.0	13.0
CM Ceramic HyperD F	50	44	46 (25–73)	>70	13.0	7.0	16.0
S Ceramic HyperD F	50	57	54 (42–75)	>70	–	–	–

General flow rate is used for pH dependence, binding strength measurements, while capacity low and high flow rates are used for dynamic capacity determinations. Mean particle size is found from coulter counting experiments and SEM pictures.

2.3.1. pH dependence measurement

pH dependence measurements were performed at pH 4.5, 5.5, 6.5, and 7.5. Sample injection was done after column equilibration followed by a NaCl gradient from 0 to 1 M during 20 CVs. A small isocratic segment corresponding to the dead volume from the pump mixing system to the injection system was part of the method. The pH dependence experiments were in most cases performed with all four-test proteins.

Retention factors, k', for the gradient runs were defined and calculated based on the retention time of the peaks:

$$k' = \frac{t_R - M_{1,0}}{M_{1,0} - M_{1,S}}$$

where t_R is the retention time of the protein, $M_{1,S}$ is the first moment of the extra column volume, and $M_{1,0}$ is the first moment of the protein at non-binding conditions found from the plate height determinations below.

2.3.2. Efficiency determination

Efficiency determinations were performed as plate height measurements at the non-binding isocratic, conditions of 1 M NaCl, pH 7.5 as a function of flow rate. Flow rates were varied between approximately 10 and 100% of the recommended maximum flow rate/pressure. The experiments were in most cases performed with all four-test proteins.

To get the best representation of the plate height, the peaks were fitted to an exponentially modified Gaussian (EMG) function using the software program TableCurve 2D ver. 2.03 from Jandel Scientific (San Rafael, CA, USA). The first and second moments were used to calculate the reduced plate height, h. The EMG function has the advantage of using the entire peak curve for the fit compared to the various graphical methods used for fitting to a Gaussian peak, and it is described as the most accurate methodology [39]. The EMG function used is a five-parameter model:

$$f(t) = \frac{A\sigma}{\tau\sqrt{2}} \exp\left[\frac{1}{2}\left(\frac{\sigma}{\tau}\right)^2 - \frac{t-\mu}{\tau}\right] \int_{-\infty}^{Z} e^{-x^2}\,dx + E,$$

$$\text{with } Z = \frac{1}{\sqrt{2}}\left(\frac{t-\mu}{\sigma} - \frac{\sigma}{\tau}\right)$$

where t is the time, A is the scaling, μ is the Gaussian mean value, σ is symmetrical peak width, τ is the asymmetrical peak width, and E is the peak base line level. Fits to the EMG function were generally performed with a correlation factor higher than 0.99. In a few difficult cases, fits to the EMG function were performed with a correlation factor down to 0.95. The first and second moments, M_1 and M_2, of the peak curve [40]:

$$M_1 = \mu + \tau$$

$$M_2 = \sigma^2 + \tau^2$$

are additive parameters, thus for an exponentially modified Gaussian peak the reduced theoretical plate height of the column, h, is found from:

$$h = \frac{H}{d_p} = \frac{L}{d_p N} = \frac{L(M_{2,0} - M_{2,S})}{d_p(M_{1,0} - M_{1,S})^2}$$

where H is the theoretical plate height, d_p is the particle diameter, L is the column length, N is the number of theoretical plates of the column, $M_{2,0}$ is the second moment of the protein peak at non-binding conditions, and $M_{2,S}$ is the second moment of the extra column volume. h in this study is presented as a function of the linear flow rate, v:

$$v = \frac{v_{vol}}{\pi r^2}$$

where v_{vol} is the volumetric flow rate and r is the column radius.

2.3.3. Binding strength measurement

Binding strength experiments were performed as the classical isocratic retention measurements as a function of NaCl concentration, which was varied between 25 and 425 mM depending on the resin and the protein. For all proteins, the binding strength experiments were performed at pH 5.5.

The best representation of data was achieved by fitting the peaks to an EMG function. The first moment of the fit was used to calculate the retention factor, k':

$$k' = \frac{M_1 - M_{1,0}}{M_{1,0} - M_{1,S}}$$

using the first moments of the extra column volume and the efficiency data at non-binding conditions for adjustment. The binding strength is illustrated by plotting k' versus reciprocal total ionic strength of the solution for elution. The total ionic strength, I_{Total}, was found from:

$$I_{Total} = 0.5 \sum_i c_i z_i^2$$

where c_i is the molar concentration and z_i is the ionic charge of the ionic species i in the solution for elution.

2.3.4. Dynamic capacity determination

Dynamic capacity was determined by frontal analysis experiments with anti-FVII Mab, aprotinin, and lysozyme. The column was equilibrated with 15 CVs of the standard buffer solution (16.7 mM MES + 16.7 mM HEPES + 16.7 mM sodium acetate) without salt at pH 5.5. Other conditions were performed according to the method described elsewhere [34]. Based on the UV signals obtained, the level of breakthrough was calculated by normalising the protein concentration with the initial protein concentration, C/C_0. The dynamic capacity at 10 and 50% breakthrough, $Q_{10\%}$ and $Q_{50\%}$, is presented in this study.

2.3.5. Static capacity determination

Static capacity was determined by batch adsorption experiments with anti-FVII Mab, aprotinin, and lysozyme. Resins were packed and equilibrated as stated previously with buffer

solution at pH 5.5. A_{280} of a 1 mg/ml protein solution was measured. Resins were poured out of the column into a beaker containing the protein solution. Based on results from dynamic capacity experiments, the total amount of protein in solution was two to three times that found per ml of resin. Solutions were left standing overnight (16–20 h) with slow agitation. A_{280} of the supernatant was measured. Assigning the difference in A_{280} to the amount of protein bound, static capacity was determined as this amount divided by the amount of resin present in the solution.

2.3.6. Particle size distribution measurement

Particle size distribution was measured by coulter counting. A few drops of resin in suspension were added to 100 ml of 0.9% NaCl solution. A preliminary counting of the solution was performed to ensure that the coincidence factor was below 10%. The final measurement was thus performed, counting more than 60,000 particles. A 280 μm i.d. orifice tube was employed for the measurements.

2.3.7. SEM pictures

Imaging was carried out on a FEI Quanta 200 scanning electron microscope at an acceleration voltage of 10 or 12.5 kV. The chamber was kept in low vacuum mode at a pressure of 0.45 Torr and a temperature of approximately 21 °C (ambient). The low vacuum mode eliminates charging of the samples and avoids the use of the conventional conductive coating. The secondary electrons from the sample collide with the water vapour in the chamber creating positive ions, which neutralise the charge build-up on the sample surface. For the SEM analysis, the colloidal resins were deposited on a conducting adhesive pad on the sample stub and evaporated as the sample chamber was pumped down.

2.3.8. Binding strength measurement of HBP

Binding strength measurements of HBP were performed in gradient elution mode. 5 cm × 0.5 cm i.d. columns of all resins were equilibrated with 10 CVs of a 16.7 mM MES + 16.7 mM HEPES + 16.7 mM sodium acetate solution, pH 7.5. 100 μl of a solution comprising 0.7 mg/ml HBP was applied, and the column was washed with 1 CV of equilibration solution. HBP was eluted by a 30 CVs linear gradient from 0 to 1.5 M NaCl in equilibration solution. Retention time of HBP for the different resins is compared by graphical presentation.

3. Results and discussion

The aim of this study is to compare a number of strong and weak cation-exchange resins with their corresponding heparin resins at similar conditions. The chromatographic resins presented in Table 2 cover a variety of functions and use from capture over intermediate purification to final purification in a down-stream process. Resins used for a capture step are characterised by having a fairly large particle size and a high binding capacity that may concentrate the target protein by removal of water and reduction of host cell proteins while avoiding column clogging by fermentation products at a high flow rate. Intermediate purification is employed for further removal of host cell proteins and some product related impurities. Resins for capture and intermediate purification in this study include SP, CM and Heparin Sepharose FF, SP, CM and Heparin Toyopearl 650m, and Heparin Ceramic HyperD M. Resins for down-stream purification steps are typically characterised by having a small particle size with high selectivity, possibly at high pressure operation. This will result in sharper peaks and higher resolution of the target protein to the related impurity, e.g., S Ceramic HyperD 20 and S and CM Ceramic HyperD F. The ion exchangers also cover a broad range of commercially available base matrix chemistries including agarose, methacrylate, and a ceramic composition of the HyperD resins. The column diameter employed in the experiments is not optimal for large particle size resins and some wall effects may have influenced results, but it was utilized to minimize protein consumption. The protein load employed in pH dependence, efficiency, and binding strength experiments was low and it is assumed that experiments were performed at linear chromatography conditions.

Results of pH dependence measurements are presented in Fig. 2. Aprotinin and lysozyme have isoelectric points well above the experimental pH range, and results in Fig. 2b and c, respectively, display the same expected trend of decreasing retention with increasing pH for all resins, however, the degree of change is fairly modest except for CM Ceramic HyperD F and S Ceramic HyperD 20. Especially for CM Ceramic HyperD F with lysozyme, the change in retention is more than twofold. The order of retention of resins is CM Ceramic HyperD F followed by S Ceramic HyperD 20 and followed by the rest of the resins with an almost identical retention behaviour. For aprotinin, CM Sepharose FF has the lowest retention, while Heparin Sepharose FF gives the lowest retention for lysozyme. Trends observed for aprotinin and lysozyme in this cation-exchange study are similar to those observed for anion exchangers with anti-FVII Mab, BSA and Lipolase [34,35], however, the retention dependence on pH are less pronounced and reversed. The pK_a of the carboxylic acid group of the weak cation exchangers is in the area of 4.5. The general recommendation of many suppliers is to run these resins above pH 6 for the complete dissociation of and binding to the carboxylic acid group on these resins, however, the highest binding was still obtained at the lowest pH for all resins, and no effect was observed for these linear measurements.

Isoelectric points of anti-FVII Mab and myoglobin are within the experimental pH range as shown in Table 2. Results of anti-FVII Mab and myoglobin are presented in Fig. 2a and d, respectively, and show the same trend of decreasing retention with increasing pH. For anti-FVII Mab a rather high retention is observed at pH 7.5 for most resins, which is above the p*I* of this protein. Though the overall charge of the protein is negative at pH 7.5, the retention experienced could be due

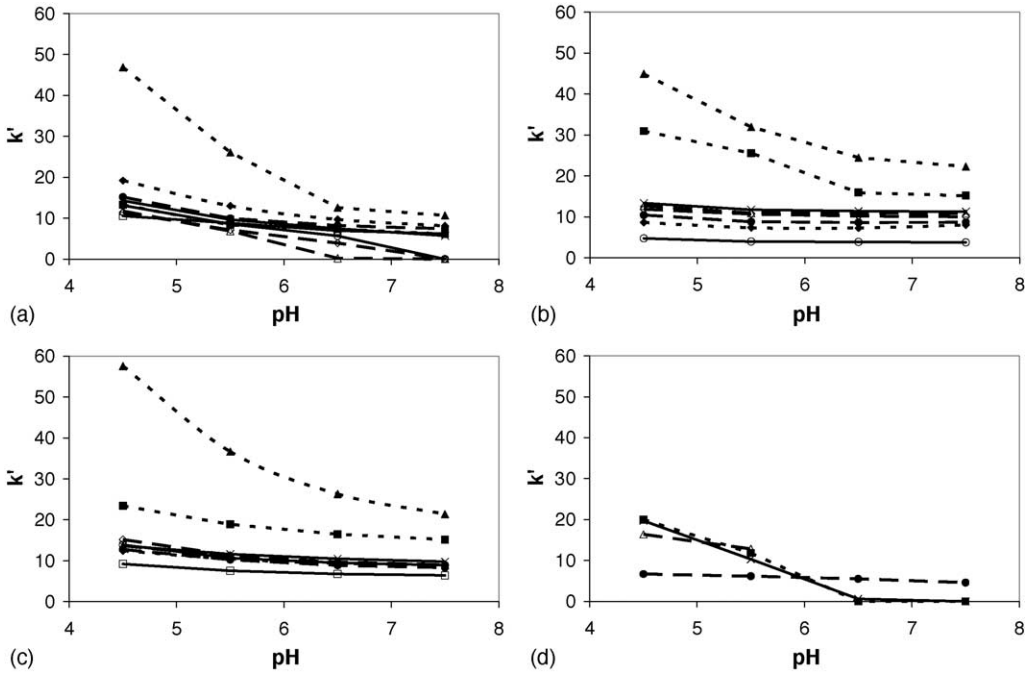

Fig. 2. pH dependence plots (k'–pH) of (a) anti-FVII Mab, (b) aprotinin, (c) lysozyme, and (d) myoglobin on cation-exchange resins. Flow rates are given in Table 2. pH dependence was determined by applying a 20 μl pulse of 1 mg/ml protein solution in 20 CVs linear gradient from 0 to 1 M NaCl in 16.7 mM MES + 16.7 mM HEPES + 16.7 mM sodium acetate buffer through a 10 cm × 0.46 cm or a 10 cm × 0.5 cm column. Symbols: ×: SP Sepharose FF, ◯: CM Sepharose FF, □: Heparin Sepharose FF, △: SP Toyopearl 650m, ◇: CM Toyopearl 650m, ●: Heparin Toyopearl 650m, ■: S Ceramic HyperD 20, ▲: CM Ceramic HyperD F, and ♦: Heparin Ceramic HyperD M.

to a local area with many positive charges. This finding is analogous to that experienced by the previous studies with anion and cation exchangers [33–35], and in general it can be stated, that a finding, concept, use or discovery working for cation-exchange chromatography will also work for anion-exchange chromatography and vice versa, which is obvious to the person skilled in the art. Essentially no binding was found for anti-FVII Mab on SP Toyopearl 650m at pH 6.5 and 7.5. For myoglobin with p*I* of this protein between 7 and 8, no binding at pH 6.5 and 7.5 were found for SP Sepharose FF and S Ceramic HyperD 20 in Fig. 2d as could be expected.

In process development, data on retention as function of pH is of great importance because a change in pH may be necessary to obtain higher buffer strength of the selected buffer system. Fig. 2 may give hints to how much or if retention would be influenced by such pH changes. Process challenge and validation issues are of great importance in the pharmaceutical industry, and these data also give an idea of pH sensitivity of resins when the pH range is established in a commercial purification process step. If a resin displays too much variation in protein retention in the selected operating pH range, it may be necessary to replace it with a less pH sensitive resin. Finally, data on retention as function of pH is useful for planning of flow-through mode operation and for step elution by increase of pH to avoid salt elution.

Fig. 3 presents the results of efficiency experiments as scaled standard van Deemter plots at unretained conditions. Resin swelling is assumed not to occur as a function of pH in the range 4.5–7.5. Fig. 3 shows the general trend of high dependence of the plate height with increasing flow rate of soft resins and there seems to be a tendency of Sepharose FF resins having steeper curves than Toyopearl 650m resins. In a few cases, scatter in the data is due to difficult and inadequate fitting to the EMG function, and because determination of h involves calculation with very small numbers which may be associated with some degree of uncertainty. The fairly high absolute values of h are a direct result of the EMG function fitting procedure fully taking the peak tailing into account compared to other fitting methods [39]. The vertical position of some resins in Fig. 3 would change if the mean particle size found in this study was used instead of supplier data (see below), and the effect would be most pronounced for the Sepharose FF resins. The trend of the curves is as expected. The trend of descending increase of h values with increasing flow rate obtained for the Ceramic HyperD resins is equal to that obtained for Q HyperD 20 [34], and could be due to size exclusion effects being dominating under non-binding conditions. Basically only the axial dispersion contribution to the reduced plate height is being measured under such conditions resulting in a relatively low flow rate dependence of the plate height. This exclusion phenomenon is previously described for gel filled porous resins by several authors, among others Farnan et al. [39] for Q HyperD F and Hunter and Carta [41] for BRX-Q.

In process development and optimisation, plate height data may be used as an indication of the purification efficiency to

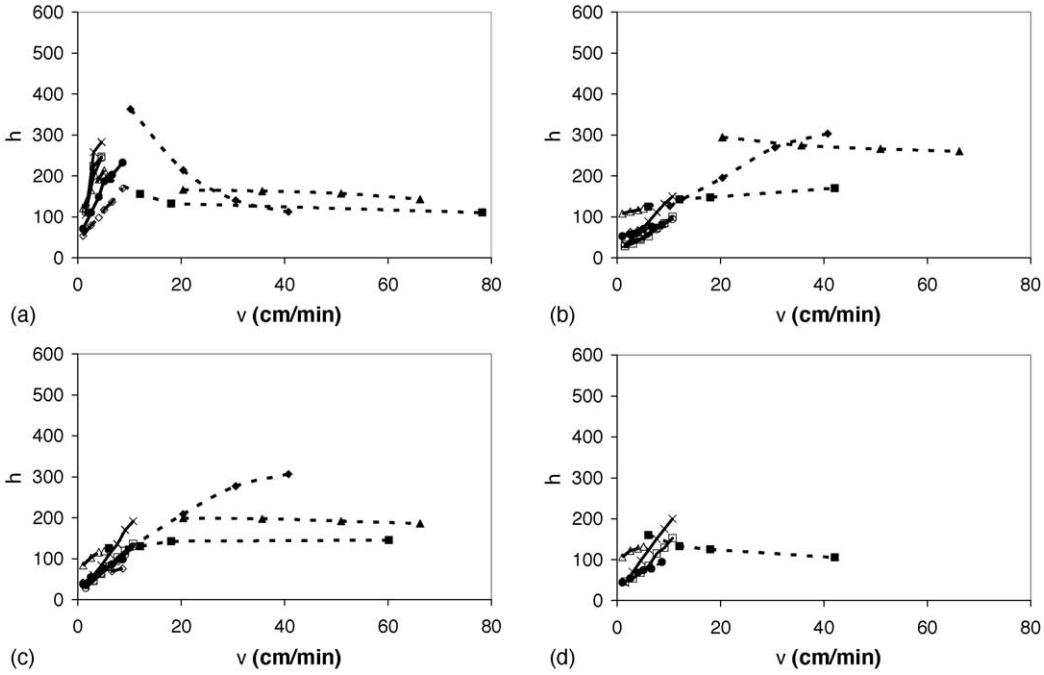

Fig. 3. Efficiency plots (h–v) of (a) anti-FVII Mab, (b) aprotinin, (c) lysozyme, and (d) myoglobin at non-binding conditions. Reduced plate height was determined by applying a 20 μl pulse of 1 mg/ml protein solution in 1 M NaCl in 16.7 mM MES + 16.7 mM HEPES + 16.7 mM sodium acetate buffer at pH 7.5 through a 10 cm × 0.46 cm or a 10 cm × 0.5 cm column. Symbols: ×: SP Sepharose FF, ◯: CM Sepharose FF, □: Heparin Sepharose FF, △: SP Toyopearl 650m, ◇: CM Toyopearl 650m, ●: Heparin Toyopearl 650m, ■: S Ceramic HyperD 20, ▲: CM Ceramic HyperD F, and ♦: Heparin Ceramic HyperD M.

be expected for the individual resins at a specified column length and flow rate, and the degree of decrease in separation as flow rate is increased. For process validation, these data will indicate the influence of a change in flow rate for a specific purification step on separation efficiency.

Particle size distribution was measured by coulter counting for unused resins. Fig. 4 shows the results, and the mean particle size (50%) is presented in Table 2. The particle size distribution for SP Sepharose FF, Heparin Toyopearl 650m, and S Ceramic HyperD 20 was not measured, but the distribution of S Ceramic HyperD F was measured and included. In general, distributions in Fig. 4a and b are broader with increase in the mean particle size. The results are in agreement (within 15%) with supplier data for most resins, however, much smaller particles were found for CM Sepharose FF and Heparin Sepharose FF. Results were verified by scanning electron microscopy (see below). The difference in results between these studies and supplier data for Sepharose resins is discussed elsewhere [33]. Results by Nash and Chase [11] on mean particle size for SP Sepharose FF are in agreement with supplier data. Finally, results on particle size distribution for Heparin Ceramic HyperD M are in agreement with results obtained by Weaver and Carta [21] on S HyperD M.

To verify particle size distribution results found by coulter counting, size distribution was measured directly on SEM pictures, see Table 2 and Fig. 5. This methodology is encumbered with depth due to measurement on a very small and possibly not representative sample, but it gives an indication of the validity of size distribution results obtained by coulter counting. Shrinkage of resins due to dehydration during SEM imaging may occur, however, a fairly good agreement of the mean particle size is obtain in Table 2 by the two independent methods (within 20%), except for Heparin Sepharose FF. The Sepharose FF and Toyopearl 650m resin SEM distribution results are in general lower than the coulter counting results possibly due to measurement on non-representative samples. The size distribution by SEM imaging in Table 2 and by coulter counting in Fig. 4 is also in fair agreement. Upon examination of Fig. 5, the structure and shape of resin particles can be observed. The three resin families are very similar in structure as expected. There are indications of some of the particles having grown together, for CM Sepharose FF and Heparin Sepharose FF maybe due to dehydration of the resins, and for Heparin Ceramic HyperD M possibly caused by the method of introducing the “gel in a shell”. Sepharose FF and Toyopearl 650m resins in Fig. 5a–e are all regular in their shape, and a more open structure of the Toyopearl 650m resins is observed, which is in agreement with the findings of Yao et al. [42] by electron tomography. The composite nature of the Ceramic HyperD resins is clearly observed in Fig. 5f–i.

Data on particle size distribution is necessary in the selection of column filter for industrial columns. If resin particles are smaller than stated or have a different shape than expected, they may clog up the filter leading to increased column backpressure and the risk of damaging column and chromatographic resin. Further, it is important to know the methodology used by suppliers to measure particle size distribution of resins in the selection of column filters if differences

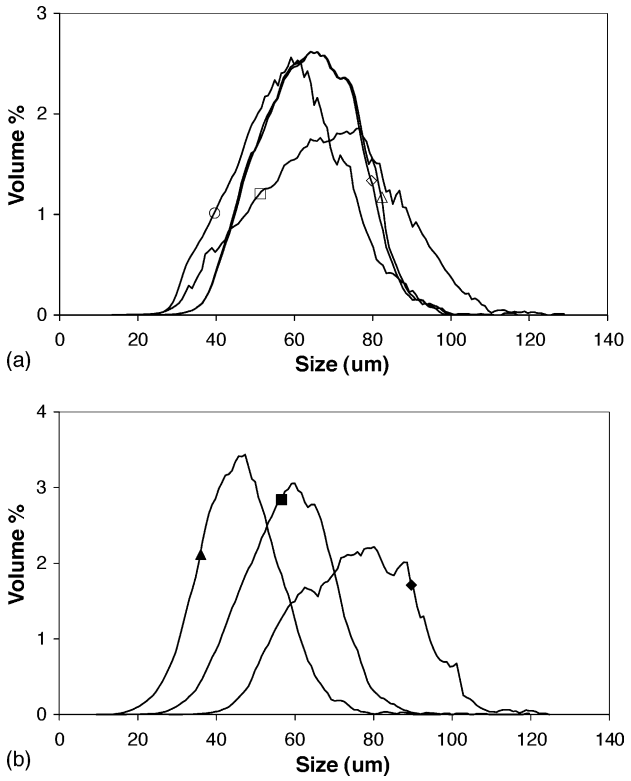

Fig. 4. Particle size distribution (%, v/v) of new anion-exchange resins in 0.9% NaCl measured by coulter counting. Symbols: (a) ◯: CM Sepharose FF, □: Heparin Sepharose FF, △: SP Toyopearl 650m, and ◇: CM Toyopearl 650m. (b) ■: S Ceramic HyperD F, ▲: CM Ceramic HyperD F, and ♦: Heparin Ceramic HyperD M.

or problems arise. In the comparison of resolution of various resins, knowledge of resin particle size is also essential. Comparison should be performed on particles of same size and distribution, and if not available, this should be taken into account upon selection of a resin for implementation in an industrial process.

Binding strength data is obtained by isocratic runs as presented in Fig. 6. Binding strength is characterised by standard k' versus I_{Total}^{-1} plots, thus stronger binding will need more salt for elution to occur and thus smaller I_{Total}^{-1}. The strongest binding of test proteins with high isoelectric point, aprotinin and lysozyme in Fig. 6b and c, is obtained for CM Ceramic HyperD F followed by S Ceramic HyperD 20, while the resin with the weakest binding is Heparin Sepharose FF a trend equal to that obtained on pH dependence measurements. Both for Ceramic HyperD and Toyopearl 650m resins, the binding strength order is CM > S/SP > Heparin, though very similar for lysozyme on CM and SP Toyopearl 650m, while for both proteins SP binds stronger than CM for Sepharose FF resins. For the three resin families and both proteins, the binding strength order is Ceramic HyperD > Toyopearl 650m > Sepharose FF for the weak cation exchangers, while the order is Ceramic HyperD > Sepharose FF > Toyopearl 650m for the strong cation exchangers. The same trend was in most cases observed for anti-FVII Mab and Lipolase on the corresponding strong anion exchangers, Q HyperD 20, Q Sepharose FF, and Toyopearl SuperQ 650s [34,35]. Retention obtained on cation exchangers is generally higher than on corresponding anion exchangers [33–35]. This is likely due to the different amino acid composition of the various solutes, and in concordance with general experience from the pharmaceutical industry. DePhillips and Lenhoff [9] have also performed extensive studies on cation-exchange resins of $\log k'$ as a function of NaCl concentration with lysozyme, α-chymotrypsinogen A, and cytochrome *c* on SP Toyopearl 650m, CM Toyopearl 650m, SP Sepharose FF, and CM Sepharose FF, and they found the same trends for binding strength as presented in this study.

The trends for the two test proteins with low isoelectric point, anti-FVII Mab and myoglobin in Fig. 6a and d, respectively, are not as clear as for aprotinin and lysozyme, but SP Toyopearl 650m is binding at the lowest salt concentration. For aprotinin, heparin resins also have a low binding strength, however, for myoglobin binding is stronger for the three heparin resins than any of the cation-exchange resins tested possibly indicating an affinity interaction occurring.

Binding strength of heparin resins is generally low as shown in Fig. 6b and c. To test the effect of binding strength on affinity interactions of heparin resins, a different protein, HBP, with well-known affinity for heparin was tested with all resins. If no affinity interaction was to occur, the most likely order of resins for binding strength should be obtained for HBP based on model results: Ceramic HyperD F > S Ceramic HyperD 20 > other resins > Heparin Sepharose FF. Fig. 7 presents the results of binding strength tests with HBP with gradient operation, which may be inspected by a simple evaluation of retention times. The elution order in Fig. 7 displays a fairly high binding strength of the three heparin resins with almost identical retention times, and only SP Sepharose FF has higher binding strength. This demonstrates a clear affinity interaction between HBP and the heparin resins, but Fig. 7 also indicates that an alternative resin possibly could be found among cation exchangers, in this case SP Sepharose FF. In fact, process development results showed (data not presented), that HBP in cultivation medium could be isolated using SP Sepharose FF with the same selectivity and purity as, and with higher capacity than heparin resins. The possible substitution of heparin resins with cation exchangers is very important for the pharmaceutical industry, because pricing of heparin resins are up to 10-fold higher and the immobilized heparin is usually derived from an animal source (porcine), both issues fairly unacceptable from economical and cGMP points of view, respectively.

Determination of binding strength is of great importance for resin selection and optimisation of industrial ion-exchange purification processes. If the protein of interest binds weakly to resins due to high loading solution conductivity and/or presence of various modifiers, etc., selection of resins for further testing should be among those to the left in Fig. 6a–d. In case of a protein generally binding strongly to all resins, a resin located to the right in Fig. 6a–d would probably

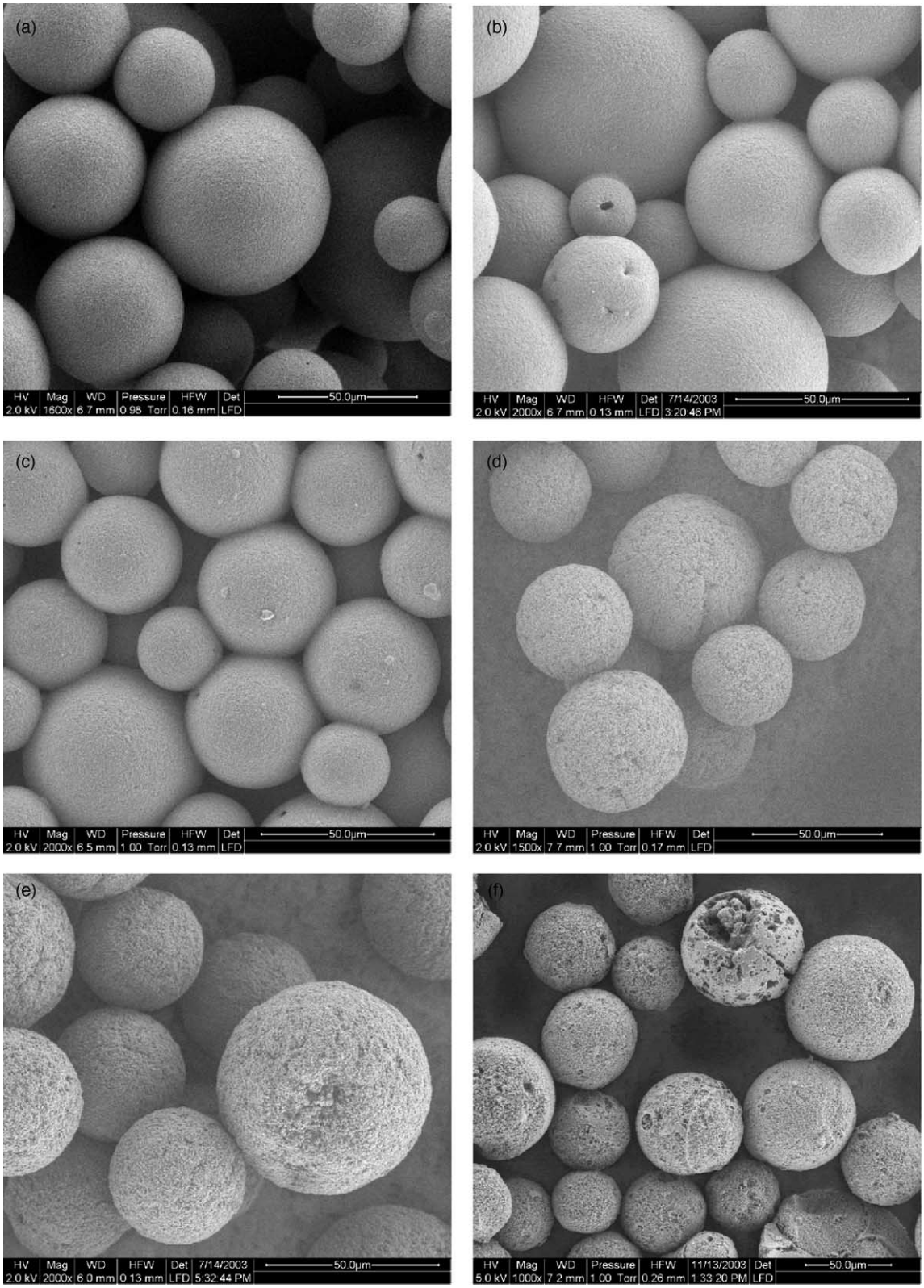

Fig. 5. SEM images of chromatographic resins at different magnification. Scale appears in the separate figures. Resins are: (a) SP Sepharose FF, (b) CM Sepharose FF, (c) Heparin Sepharose FF, (d) SP Toyopearl 650m, (e) CM Toyopearl 650m, (f) S Ceramic HyperD F, (g) S Ceramic HyperD 20, (h) CM Ceramic HyperD F, and (i) Heparin Ceramic HyperD M.

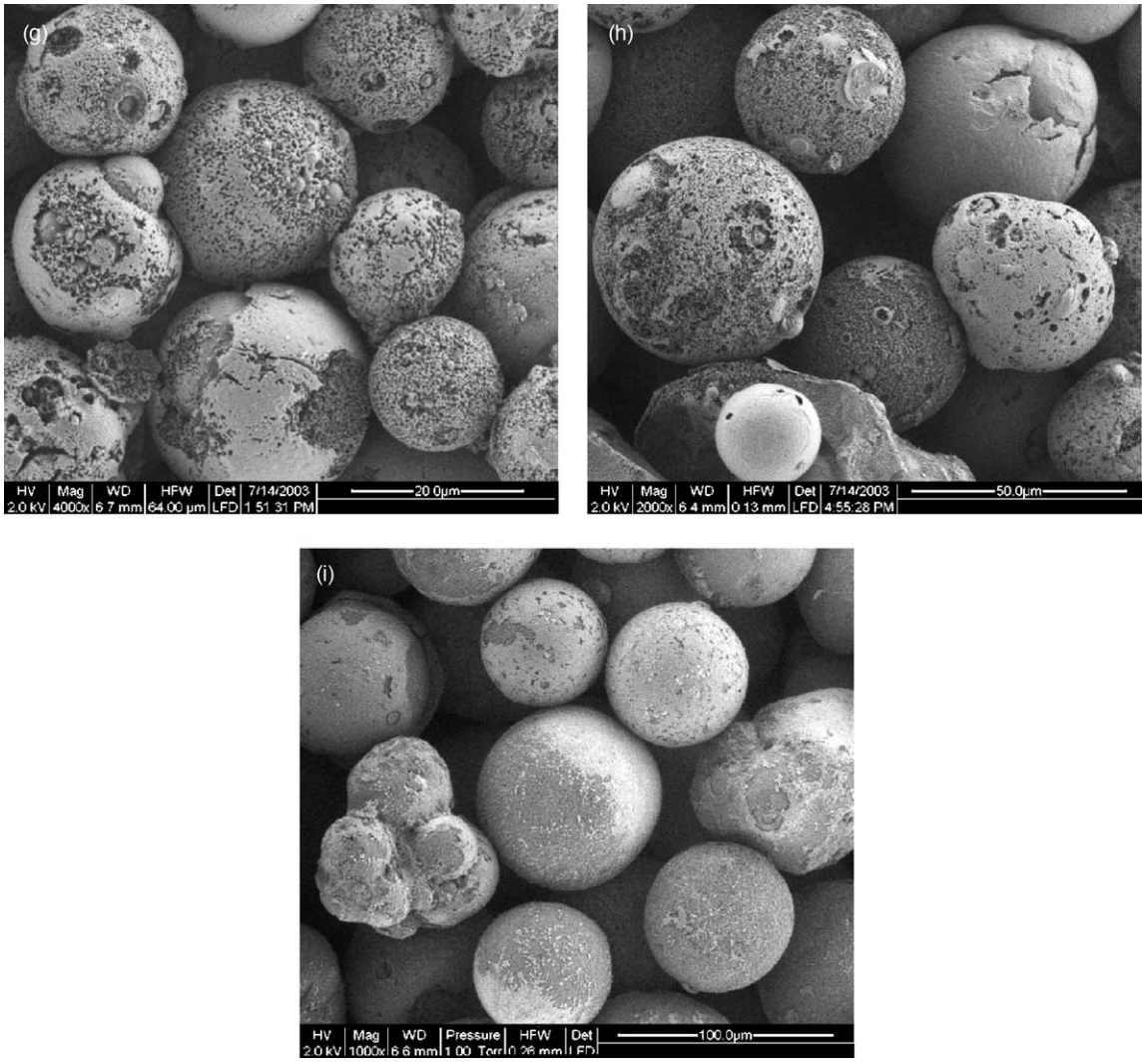

Fig. 5. (*Continued*).

be selected for further testing to minimize salt consumption or to avoid pH changes for elution. During removal of impurities in chromatographic flow-through mode operation, the target protein passes through the column, which retains the impurities preferably at the conditions of the loading sample. For this purpose resins to the right in Fig. 6a–d may also apply.

Dynamic binding capacities are determined by frontal analysis of pure proteins, and 10 and 50% breakthrough data ($Q_{10\%}$ and $Q_{50\%}$) for anti-FVII Mab, aprotinin, and lysozyme are presented in Table 3 and compared to a few dynamic capacity data for lysozyme obtained by suppliers. The purpose of this study was to monitor the influence of a fairly high and fairly low flow rate on resin performance. Applied flow rates are given in Table 2. The expected trend of slightly higher dynamic capacity at the lower flow rate compared to the higher flow rate is presented in Table 3 for all proteins. For lysozyme on S Ceramic HyperD 20, however, the highest dynamic capacity was found at the high flow rate, and we have no explanation for this result. For Sepharose FF resins, $Q_{10\%}$ and $Q_{50\%}$ were generally much higher at low flow rate compared to high flow rate due to poor mass transfer into resins particles. This is particularly distinct for lysozyme. The measurements were performed at pH 5.5 which is close to the pK_a of the carboxyl group ligand of the weak cation exchangers, and outside the recommended pH working range of resins like CM Sepharose FF. This could influence both binding strength and capacity results of weak cation exchangers, however, no indication of that was obtained. In fact, the capacity of CM Ceramic HyperD F was higher than of S Ceramic HyperD 20 for aprotinin and lysozyme, and a similar pattern was to some extent obtained for Sepharose FF and Toyopearl 650m resins. The higher capacity of CM Ceramic HyperD F is probably due to the higher ionic capacity compared to S Ceramic HyperD 20, ionic capacities being $\geq$250 and $\geq$150 μeq/ml, respectively. Good agreement was obtained between this study and the few supplier data available for lysozyme, that is for SP Toyopearl 650m, CM Toyopearl 650m, and S Ceramic HyperD

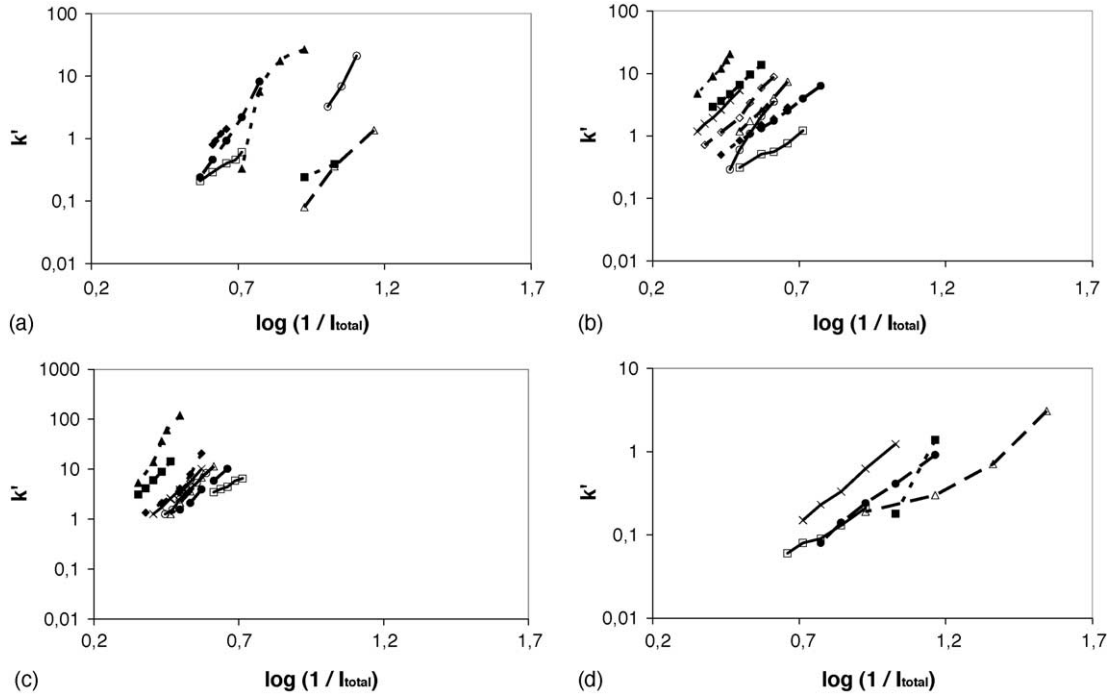

Fig. 6. Binding strength plots (k'–I_{Total}^{-1}) at pH 5.5 of (a) anti-FVII Mab, (b) aprotinin, (c) lysozyme, and (d) myoglobin on cation-exchange resins at approximately 50% of recommended maximum operating flow rate. Actual flow rates are given in Table 2. Binding strength was determined by applying a 20 μl pulse of 1 mg/ml protein solution in 16.7 mM MES + 16.7 mM HEPES + 16.7 mM sodium acetate at various isocratic NaCl concentrations through a 10 cm × 0.46 cm or a 10 cm × 0.5 cm column. Symbols: ×: SP Sepharose FF, ◯: CM Sepharose FF, □: Heparin Sepharose FF, △: SP Toyopearl 650m, ◇: CM Toyopearl 650m, ●: Heparin Toyopearl 650m, ■: S Ceramic HyperD 20, ▲: CM Ceramic HyperD F, and ♦: Heparin Ceramic HyperD M.

20. Results for lysozyme with SP Sepharose FF are in good agreement with the slightly higher outcome (140 mg/ml) obtained by Nash and Chase [11] using a protein concentration of 2 mg/ml, however, results obtained for IgG on the same resin differ by a factor of 10. This is likely due to different properties for the two IgGs, as the dynamic capacity of anti-FVII Mab on all cation exchangers is generally low, as often experienced with IgG. Hahn et al. [24] found the dynamic capacity ($Q_{10\%}$) of a pure IgG solution at pH 4.7 on SP Sepharose FF to be approximately 7 mg/ml at a flow rate below the flow rates employed in this study. Thus, their result is in very good agreement with data obtained from this study although the characteristics of the two IgGs may differ.

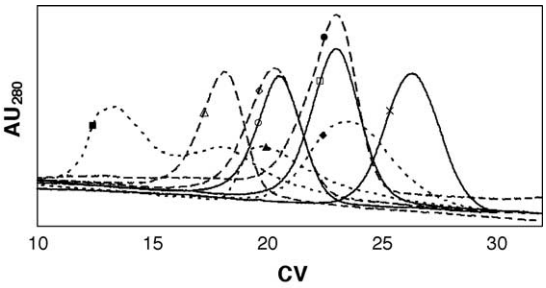

Fig. 7. Retention of HBP in a linear NaCl gradient from 0 to 1.5 M over 30 CVs. Solvent system is 16.7 mM MES + 16.7 mM HEPES + 16.7 mM sodium acetate, pH 7.5. Symbols: ×: SP Sepharose FF, ◯: CM Sepharose FF, □: Heparin Sepharose FF, △: SP Toyopearl 650m, ◇: CM Toyopearl 650m, ●: Heparin Toyopearl 650m, ■: S Ceramic HyperD 20, ▲: CM Ceramic HyperD F, and ♦: Heparin Ceramic HyperD M.

Static capacity results obtained with a 1 mg/ml solution of lysozyme are shown in Table 3. Data was not measured for all resins. Static capacity is considered the maximum possible capacity that can be obtained for a specific resin at the given conditions. By comparison with dynamic capacity data at 10% breakthrough an indication of the fraction of the column utilized during preparative operation is obtained. Excluding the result of CM Sepharose FF, the fraction utilized at 10% breakthrough range within 40–80% for either flow rate; lowest for CM Ceramic HyperD F and highest for CM Toyopearl 650m. A high degree of dependence of dynamic capacity on flow rate is obtained for CM Ceramic HyperD F, Heparin Toyopearl 650m, and to some extent for Heparin Ceramic HyperD M. This indicates that a different degree of improved productivity of the resins may be obtained in process development by decreasing flow rate compared to this study. Chang and Lenhoff [18] obtained the static capacity result of 92 mg/ml with SP Sepharose FF at pH 7 and 0.1 M NaCl for a 3 mg/ml lysozyme solution. This result is as expected slightly lower than the dynamic results of this study due to the higher salt concentration of their experimental setup and thus in very good agreement. Levison et al. [8] also measured static capacity for SP Sepharose FF, CM Sepharose FF, SP Toyopearl 650m, CM Toyopearl 650m, and S HyperD M and the results are given in Table 3. As presented in Table 3, a

Table 3
Binding capacity of heparin and cation-exchange resins for 1 mg/ml solutions of anti-FVII Mab, lysozyme, and aprotinin

Resin	Dynamic capacity Q, % breakthrough, anti-FVII Mab (mg/ml)				Dynamic capacity Q, % breakthrough, aprotinin (mg/ml)				Dynamic capacity Q, % breakthrough, lysozyme (mg/ml)				Dynamic capacity obtained by the suppliers, lysozyme (mg/ml)	Static capacity, lysozyme (mg/ml)	Static capacity of Levison et al. [8], lysozyme (mg/ml)
	Low flow rate		High flow rate		Low flow rate		High flow rate		Low flow rate		High flow rate				
	$Q_{10\%}$	$Q_{50\%}$	$Q_{10\%}$	$Q_{50\%}$	$Q_{10\%}$	$Q_{50\%}$	$Q_{10\%}$	$Q_{50\%}$	$Q_{10\%}$	$Q_{50\%}$	$Q_{10\%}$	$Q_{50\%}$			
Heparin Sepharose FF	6	8	3	6	8	9	7	9	4	5	3	4	–	–	–
SP Sepharose FF	8	16	6	15	79	84	76	81	104	110	87	97	–	–	131
CM Sepharose FF	–	–	–	–	–	–	–	–	136	155	45	84	–	93	106
Heparin Toyopearl 650m	–	–	–	–	–	–	–	–	17	20	17	21	–	29	–
SP Toyopearl 650m	–	–	–	–	–	–	–	–	–	–	30	42	40–60	45	47
CM Toyopearl 650m	–	–	4	4	40	41	34	36	41	44	41	44	35–55	52	44
Heparin Ceramic HyperD M	27	39	12	21	14	16	10	13	20	24	13	20	–	28	–
S Ceramic HyperD 20	–	–	–	–	110	118	110	114	98	110	114	123	≥85	–	110[a]
CM Ceramic HyperD F	–	–	14	15	134	160	118	155	–	–	126	151	–	261	–

Dynamic capacity results are determined at 10 and 50% breakthrough, $Q_{10\%}$ and $Q_{50\%}$, at flow rates of approximately 25 and 75% of recommended maximum operating flow rate/pressure. Flow rates are presented in Table 2.
[a] Results obtained on S HyperD M.

general good agreement is obtained between the two studies, though the capacity order of SP Toyopearl 650m and CM Toyopearl 650m is slightly reversed. Nakamura et al. [5] found static capacities of anti-thrombin III to be 5–6 mg/ml for the three heparin resins of this study. The ligand densities of the three heparin resins are within the range 5–10 mg heparin/ml resin corresponding to ionic capacities below 100 μeq/ml and much below the ionic capacities of the ion exchangers. This is likely why the heparin resins have low capacities both as affinity resins and just regarded as ion exchangers.

Binding capacity data is very important to the industry. In cases where process economy is a constraint or if two or more resins during process development perform equally well with respect to resolution, flow rate, price, etc., the resin with the highest capacity will be chosen for the production process to increase productivity. Binding capacities of true mixtures such as fermentation broth give a more realistic picture of what to expect in the initial process development situation [43], however, binding capacity was measured for pure proteins in this study, because supply of uniform fermentation broth is difficult to obtain and store through a long period of time. Results for pure proteins should thus be used only for selection of a few appropriate resins for further testing and optimization for the specific objective.

4. Conclusion

A comparative study was performed with model proteins on strong and weak cation exchangers and their corresponding heparin resins for a number of chromatographic parameters. A general good agreement was obtained between this study and data obtained by others. The effect of binding strength on affinity actions of heparin resins was tested using HBP, and a distinct difference was obtained compared to model proteins like lysozyme. Thus, heparin resins may be used as cation exchangers, but should only be employed as an affinity resin to purify corresponding proteins, as expected. Results also showed that very high binding strength may be achieved with HBP on an ordinary cation exchanger that could substitute the more expensive heparin resin, in this case on SP Sepharose FF.

Data generated in this study should be used for selection of resins for further testing in process development. However, the data cannot be used to estimate selectivity differences or resolution between target proteins and specific impurities. None of the resins should be regarded as good or poor for chromatographic operation but more or less suitable for a specific purpose, and only testing for the specific application will determine which resin is optimal.

5. Nomenclature

A	scaling parameter
A_{280}	absorbance at 280 nm

c_i	molar concentration of component *i*
C/C_0	normalised protein concentration
CVs	column volumes
E	base line level
EMG	exponentially modified Gaussian
I_{Total}	total ionic strength
k'	retention factor
M_1	first moment of the peak curve
M_2	second moment of the peak curve
$M_{1,S}$	first moment of the extra column volume
$M_{2,S}$	second moment of the extra column volume
$M_{1,0}$	first moment of the unretained protein
$M_{2,0}$	second moment of the unretained protein
v	linear flow rate
v_{vol}	volumetric flow rate
Z	dummy parameter
z_i	ionic charge of component *i*

Greek symbols

μ	Gaussian mean retention time
σ	symmetrical peak width
τ	asymmetrical peak width

Acknowledgements

The supply of Novo Nordisk proteins from Claus Rix Melchiorsen, Birgitte Silau, and Ole Elvang Jensen, and set up of dynamic capacity measurements and EMG data fitting procedures from Ulrik Borgbjerg are gratefully acknowledged. A special acknowledgement to Randi Holm Jensen for performing a lot of the data handling and to Bjørn Bentzen for providing the heparin structure in Fig. 1.

References

[1] M. Lindsay, G.-C. Gil, A. Cadiz, W.H. Velander, C. Zhang, K.E. Van Cott, J. Chromatogr. A 1026 (2004) 149.
[2] A. Heger, T. Grunert, P. Schulz, D. Josic, A. Buchacher, Thromb. Res. 106 (2002) 157.
[3] G. Garke, W.-D. Deckwer, F.B. Anspach, J. Chromatogr. B 737 (2000) 25.
[4] K. Karlsson, N. Cairns, G. Lubec, M. Fountoulakis, Electrophoresis 20 (1999) 2970.
[5] K. Nakamura, A. Sakane, M. Hasegawa, Y. Kato, K. Sekizawa, H. Sasaki, K. Inouye, Presented at the Affinity Interactions Conference, Cambridge, UK, 2003, Poster.
[6] P. DePhillips, A.M. Lenhoff, J. Chromatogr. A 883 (2000) 39.
[7] E. Boschetti, J. Chromatogr. A 658 (1994) 207.
[8] P. Levison, C. Mumford, M. Streater, A. Brandt-Nielsen, N.D. Pathirana, S.E. Badger, J. Chromatogr. A 760 (1997) 151.
[9] P. DePhillips, A.M. Lenhoff, J. Chromatogr. A 933 (2001) 57.
[10] R. Noel, G. Proctor, Presented at Recovery of Biological Products X, Cancun, Mexico, June 2001, Poster.
[11] D.C. Nash, H.A. Chase, J. Chromatogr. A 807 (1998) 185.
[12] J. Horvath, E. Boschetti, L. Guerrier, N. Cooke, J. Chromatogr. A 679 (1994) 11.
[13] S. Yamamoto, T. Ishihara, J. Chromatogr. A 852 (1999) 31.
[14] S. Yamamoto, E. Miyagawa, J. Chromatogr. A 852 (1999) 25.
[15] J. Renard, C. Vidal-Madjar, B. Sebille, J. Liq. Chromatogr. 15 (1992) 71.
[16] L. Dunn, M. Abouelezz, L. Cummings, M. Navvab, C. Ordnez, C.J. Siebert, K.W. Talmadge, J. Chromatogr. 548 (1991) 165.
[17] M. McCoy, K. Kalghatgi, F.E. Regnier, N. Afeyan, J. Chromatogr. A 743 (1996) 221.
[18] C. Chang, A.M. Lenhoff, J. Chromatogr. A 827 (1998) 281.
[19] Y.-B. Yang, K. Harrison, J. Kindsvater, J. Chromatogr. A 723 (1996) 1.
[20] M. Weitzhandler, D. Farnan, J. Horvath, J.S. Rohrer, R.W. Slingsby, N. Avdalovic, C. Pohl, J. Chromatogr. A 828 (1998) 365.
[21] L.E. Weaver, G. Carta, Biotechnol. Prog. 12 (1996) 342.
[22] Y. Hu, P.W. Carr, Anal. Chem. 70 (1998) 1934.
[23] M.A. Hashim, K.-H. Chu, P.-S. Tsan, J. Chem. Tech. Biotechnol. 62 (1995) 253.
[24] R. Hahn, P.M. Schulz, C. Schaupp, A. Jungbauer, J. Chromatogr. A 795 (1998) 277.
[25] C.M. Roth, K.K. Unger, A.M. Lenhoff, J. Chromatogr. A 726 (1996) 45.
[26] F. Fang, M.-I. Aguilar, M.T.W. Hearn, J. Chromatogr. A 729 (1996) 67.
[27] C.B. Mazza, S.M. Cramer, J. Liq. Chromatogr. Rel. Technol. 22 (1999) 1733.
[28] K. Hamaker, S.-L. Rau, R. Hendrickson, J. Liu, C.M. Ladisch, M.R. Ladisch, Ind. Eng. Chem. Res. 38 (1999) 865.
[29] V. Natarajan, S.M. Cramer, J. Chromatogr. A 876 (2001) 63.
[30] V. Natarajan, S. Cramer, Sep. Sci. Technol. 35 (2000) 1719.
[31] P. DePhillips, A.M. Lenhoff, J. Chromatogr. A 1036 (2004) 51.
[32] C.B. Mazza, N. Sukumar, C.M. Breneman, S.M. Cramer, Anal. Chem. 73 (2001) 5457.
[33] A. Staby, M.-B. Sand, R.G. Hansen, J.H. Jacobsen, L.A. Andersen, M. Gerstenberg, U.K. Bruus, I.H. Jensen, J. Chromatogr. A 1034 (2004) 85.
[34] A. Staby, I.H. Jensen, I. Mollerup, J. Chromatogr. A 897 (2000) 99.
[35] A. Staby, I.H. Jensen, J. Chromatogr. A 908 (2001) 149.
[36] L. Thim, S. Bjørn, M. Christensen, E.M. Nicolaisen, T. Lund-Hansen, A.H. Pedersen, U. Hedner, Biochemistry 27 (1988) 7785.
[37] H. Fritz, G. Wunderer, Arzneim. Forsch./Drug Res. 33 (1983) 479.
[38] H. Flodgaard, E. Østergaard, S. Bayne, A. Svendsen, J. Thomsen, M. Engels, A. Wollmer, Eur. J. Biochem. 197 (1991) 535.
[39] D. Farnan, D.D. Frey, C. Horvath, Biotechnol. Prog. 13 (1997) 429.
[40] E. Grushka, Anal. Chem. 44 (1972) 1733.
[41] A.K. Hunter, G. Carta, J. Chromatogr. A 897 (2000) 65.
[42] Y. Yao, K. Czymmek, M.R. Shure, A.M. Lenhoff, Presented at PREP'2004, Baltimore, MD, 22–26 May 2004, Poster.
[43] A. Staby, N. Johansen, H. Wahlstrøm, I. Mollerup, J. Chromatogr. A 827 (1998) 311.